Synthesis, Characterization, and Molecular Structure of the Quadruply Bonded Ditungsten(II) Complex, $W_2Cl_4(dppm)_2$

JO ANN M. CANICH and F. ALBERT COTTON

Department of Chemistry and Laboratory for Molecular Structure and Bonding, Texas A and M University, College Station, Tex. 77843, U.S.A.

(Received April 29, 1987)

Abstract

The reaction of $W_2Cl_4[P(n\text{-}Bu)_3]_4$ with bis(diphenylphosphino)methane (dppm) affords the highly air-sensitive material, $W_2Cl_4(dppm)_2$, which has been characterized by IR and visible spectroscopy, and by X-ray crystallography. The compound crystallizes in the centrosymmetric space group $C2/c$ with the following parameters: $a = 17.298(3)$; $b = 17.011(2)$; $c = 18.413(2)$ Å; $\beta = 98.93(2)$; $V = 5352(2)$ Å^3; $Z = 4$. The molecule is positioned about a C_2 axis which allows for a net torsion angle of 17.25° down the W–W vector. This does not seem to significantly effect the W–W bond distance (2.269(1) Å) relative to other quadruply bonded ditungsten species.

Introduction

While there are multiple synthetic routes to quadruply bonded molybdenum $M_2Cl_4(L\text{–}L)_2$ compounds [1] where L–L is a chelating or bridging bidentate phosphine ligand, the analogous tungsten chemistry is quite limited. In fact, the only synthetic avenue to such compounds involves the substitution of bidentate phosphine ligands from compounds containing monodentate phosphine ligands, L

$$W_2Cl_4L_4 + 2L\text{–}L \longrightarrow W_2Cl_4(L\text{–}L)_2 + 4L$$

To date, only three such compounds have been prepared in this manner, namely α- and β-$W_2Cl_4(dppe)_2$ and α-$W_2Cl_4(dmpe)_2$ (dppe = 1,2-bis(diphenylphosphino)ethane, dmpe = 1,2-bis(dimethylphosphino)ethane) [2]. We would now like to report the successful preparation and structural characterization of $W_2Cl_4(dppm)_2$ (dppm = bis(diphenylphosphino)methane using a similar synthetic route, and in addition the attempted preparation of $W_2Cl_4(dppm)_2$ via tungsten(II) carboxylates.

Experimental

All manipulations were carried out under an atmosphere of argon unless otherwise specified. Standard Schlenk and vacuum line techniques were used. Commercial grade solvents were freshly distilled from benzophenone ketyl prior to use. $W_2Cl_4[P(n\text{-}Bu)_3]_4$ [2] and $W_2(O_2CPh)_4$ [3] were prepared by literature methods involving the reduction of WCl_4 with sodium amalgam in the presence of either tri-n-butylphosphine $P(n\text{-}Bu)_3$ or sodium benzoate. The compound $W_2Cl_4[P(n\text{-}Bu)_3]_4$ was further purified by passing an air-stable hexane solution down a column packed with Kieselgel 60 (American Scientific, Chromatin Div.). Bis(diphenylphosphino)-methane (dppm) and trimethylsilyl chloride were purchased from Aldrich Chemical Co. and used without further purification. The IR and visible spectra were recorded on a Perkin-Elmer 783 spectrophotometer and a Cary 17D spectrophotometer, respectively.

Preparation of $W_2Cl_4(dppm)_2$

To a 250 ml round bottom flask with side arm and attached reflux condenser, 2.249 g (1.71 mmol) of $W_2Cl_4[P(n\text{-}Bu)_3]_4$, 1.36 g (3.54 mmol) of dppm, 30 ml of toluene and 60 ml of hexane were added. The reaction was stirred and refluxed for 4 h to give a light brown microcrystalline solid and a blue–green solution containing unreacted starting material, in addition to $P(n\text{-}Bu)_3$. The solid was filtered from the solution, washed with two 10 ml aliquots of hexane and vacuum dried to give a 50% yield of $W_2Cl_4(dppm)_2$. This reaction also proceeds in the presence of water. In a 100 ml round bottom Schlenk flask with attached reflux condenser, 0.10 g (0.076 mmol) $W_2Cl_4[P(n\text{-}Bu)_3]_4$ and 0.064 g (0.17 mmol) dppm were dissolved in 10 ml hexane. Deaerated deionized water (20 μl) was added and the reaction mixture was refluxed for 3 h. Upon filtration and washing with hexane, $W_2Cl_4(dppm)_2$ was recovered in a 42% yield. IR (Nujol, CsI) cm^{-1}: 1585(vw), 1574(w), 1484(m), 1437(s), 1332(vw), 1306(vw), 1276(vw), 1190(w), 1163(w), 1145(vw), 1127(m), 1103(m), 1095(m), 1075(w), 1030(w), 1002(w), 847(w), 800(s), 766(m), 761(m), 750(m), 740(s), 729(m), 697(s), 622(w), 525(s), 512(s), 496(ms), 486(ms), 465(m), 430(m), 419(m), 383(w), 354(w),

0020-1693/88/$3.50

330(s), 304(m). Visible (benzene) nm: 367(s), 407(s), 496(m), 737(s). Visible (Nujol mull) nm: 380(s), 486(m), 726(m).

Reaction of $W_2(O_2CPh)_4$ with dppm and Me_3SiCl

To a 100 ml round bottom flask with side arm and attached reflux condenser, 0.50 g (0.51 mmol) $W_2(O_2CPh)_4 \cdot 2thf$, 0.393 g (1.02 mmol) dppm and 30 ml toluene were added. The reaction mixture was stirred while 250 μl (1.97 mmol) of trimethylsilyl chloride was slowly added. Upon gentle heating for 1 h, a red solution was generated which gave a characteristic visible spectrum (496 nm). No attempt was made to further characterize this solution.

Reaction of $W_2Cl_4(dppm)_2$ with Me_3SiCl

In a 100 ml round bottom Schlenk flask, 0.10 g (0.08 mmol) $W_2Cl_4(dppm)_2$ was dissolved in 20 ml of toluene. Me_3SiCl (12 μl, 0.09 mmol) was added to this, and the reaction mixture was briefly heated (3 min) and stirred (12 h). A red solution resulted which gave a similar visible spectrum (498 nm) to that found for the previous reaction. No attempt was made to further characterize the red solution produced in this reaction.

Crystallographic Study

Red–green dichroic crystals of $W_2Cl_4(dppm)_2$ were readily grown by dissolving 0.05 g of the microcrystalline brown solid in 10 ml of toluene, and then carefully layering the solution with 10 ml of hexane, thus allowing for slow diffusion between solvent layers. X-ray crystallographic quality crystals were grown by this method in less than one day.

The geometric and intensity data were gathered with an automated four-circle Syntex P1 diffractometer, using a crystal mounted in a glass capillary tube with epoxy. Routine unit cell identification and intensity data collection procedures have been described previously [4]. Axial photographs of the principal axes and the c-diagonal were taken to verify lattice dimensions and c-centering for the monoclinic cell. Systematic absences in the intensity data narrowed the choice of space groups between $C2/c$ and Cc. Polarization, Lorentz and empirical absorption corrections based on azimuthal scans of nine reflections were applied to the intensity data. The position of the unique tungsten atom was determined from the Patterson map and the centrosymmetric space group was chosen and found to be correct. The remaining non-hydrogen atoms were located by a series of difference maps and least-squares refinements using the Enraf-Nonius Structure Determination Package of programs. No attempt was made to locate and refine the hydrogen atoms. All atoms with the exception of those from the solvent molecule were refined anisotropically. Final anisotropic refinement converged to $R = 0.03288$ ($R_w = 0.04493$) and the largest peak on the difference Fourier map following refinement was 0.742 e/Å^3. Additional crystallographic parameters for the data collection and structure refinement are given in Table I, fractional atomic coordinates are in Table II, and relevant bond distances and angles are in Table III. An ORTEP view of $W_2Cl_4(dppm)_2$ is shown in Fig. 1, and defines the atomic numbering scheme used in the Tables.

TABLE I. Crystal Data for $W_2Cl_4(dppm)_2 \cdot C_7H_8$

Formula	$W_2Cl_4P_4C_{57}H_{57}$
Formula weight	1370.46
Space group	$C2/c$
Systematic absences	hkl $(h+k \neq 2n)$; $h0l$ $(l \neq 2n)$
a (Å)	17.298(3)
b (Å)	17.011(2)
c (Å)	18.413(2)
β (°)	98.93(2)
V (Å^3)	5352(2)
Z	4
D_{calc} (g/cm^3)	1.707
Crystal size (mm)	0.6 × 0.5 × 0.4
μ(Mo Kα) (cm^{-1})	47.627
Data collection instrument	Syntex P$\bar{1}$
Radiation (monochromated in incident beam)	Mo Kα (λ_α = 0.71073 Å)
Orientation reflections, number, range (2θ)	15, $21.41 \leq 2\theta \leq 30.4$
Temperature (°C)	0
Scan method	$\omega - 2\theta$
Data col. range, 2θ (°)	$4 \leq 2\theta \leq 45$
No. unique data, total with $F_o^2 > 3\sigma(F_o^2)$	3506, 2665
Number of parameters refined	295
Transmission factors, max./min.	0.9989/0.8840
R[a]	0.03288
R_w[b]	0.04493
Quality-of-fit indicator[c]	0.989
Largest shift/e.s.d., final cycle	0.00
Largest peak (e/Å^3)	0.742

[a] $R = \Sigma||F_o| - |F_c||/\Sigma|F_o|$. [b] $R_w = [\Sigma w(|F_o| - |F_c|)^2/\Sigma w|F_o|^2]^{1/2}$; $w = 1/\sigma^2(|F_o|)$. [c] Quality-of-fit = $[\Sigma w(|F_o| - |F_c|)^2/(N_{obs} - N_{parameters})]^{1/2}$.

Results and Discussion

Synthesis

Compared with compounds containing a Mo_2^{4+} core, the W_2^{4+} core species are more easily oxidized. This general relationship has been studied by a combination of photoelectron spectroscopy and molecular quantum mechanics [5], and is also manifested in solution by the lower oxidation potential of $W_2Cl_4(PR_3)_4$ to $[W_2Cl_4(PR_3)_4]^+$ than of $Mo_2Cl_4(PR_3)_4$ to $[Mo_2Cl_4(PR_3)_4]^+$ [2, 6]. Thus, it is not surprising

TABLE II. Atomic Positional Parameters and Equivalent Isotropic Displacement Parameters for $W_2Cl_4(dppm)_2 \cdot C_7H_8$[a]

Atom	x	y	z	B (Å²)[b]
W	0.46783(2)	0.21391(2)	0.19139(2)	2.249(6)
Cl(1)	0.5736(1)	0.3459(1)	0.3353(1)	3.24(5)
Cl(2)	0.5503(1)	0.0822(1)	0.3506(1)	3.92(5)
P(1)	0.4109(1)	0.2501(1)	0.3699(1)	2.56(5)
P(2)	0.6666(1)	0.1939(1)	0.2745(1)	2.66(5)
C(1)	0.6758(5)	0.2650(5)	0.2016(5)	2.6(2)
C(2)	0.6189(5)	0.1799(5)	0.0648(5)	3.0(2)
C(3)	0.6966(6)	0.1742(7)	0.0519(6)	4.8(2)
C(4)	0.7150(7)	0.1177(8)	0.0019(7)	6.5(3)
C(5)	0.6581(8)	0.0686(8)	−0.0344(8)	7.4(3)
C(6)	0.5809(7)	0.0768(7)	−0.0249(6)	6.0(3)
C(7)	0.5609(6)	0.1321(7)	0.0260(6)	4.4(2)
C(8)	0.5881(5)	0.3432(5)	0.0793(5)	2.9(2)
C(9)	0.6060(6)	0.4134(6)	0.1165(6)	4.0(2)
C(10)	0.6104(7)	0.4834(7)	0.0775(7)	5.4(3)
C(11)	0.5930(7)	0.4844(7)	0.0018(7)	5.4(3)
C(12)	0.5732(7)	0.4143(7)	−0.0363(6)	5.4(3)
C(13)	0.5727(6)	0.3428(6)	0.0016(5)	4.0(2)
C(14)	0.2540(5)	0.2147(5)	0.1501(5)	3.1(2)
C(15)	0.2540(6)	0.1718(6)	0.0849(5)	3.6(2)
C(16)	0.1932(6)	0.1784(7)	0.0278(6)	4.6(3)
C(17)	0.1316(6)	0.2312(6)	0.0339(6)	4.5(2)
C(18)	0.1299(7)	0.2723(7)	0.0978(6)	5.4(3)
C(19)	0.1926(6)	0.2661(6)	0.1571(6)	3.9(2)
C(20)	0.3001(5)	0.1026(5)	0.2622(5)	2.9(2)
C(21)	0.2191(6)	0.0886(6)	0.2602(6)	4.0(2)
C(22)	0.1752(6)	0.0220(6)	0.2944(6)	4.4(2)
C(23)	0.2474(6)	−0.0325(6)	0.3286(6)	4.9(3)
C(24)	0.3271(7)	−0.0186(7)	0.3292(7)	5.6(3)
C(25)	0.3537(6)	0.0475(5)	0.2939(6)	4.2(2)
C(26)	0.500	0.282(1)	0.750	8.3(6)*
C(27)	0.426(1)	0.265(1)	0.691(1)	5.2(5)*
C(28)	0.402(2)	0.197(1)	0.673(1)	5.9(6)*
C(29)	0.442(2)	0.135(2)	0.713(2)	8.4(8)*
C(30)	0.500	0.138(2)	0.750	10.2(7)*
C(31)	0.536(2)	0.216(2)	0.784(2)	7.7(7)*
C(32)	0.504(7)	0.371(3)	0.765(4)	17(1)*

[a]e.s.d.s given in parentheses. [b]Anisotropically refined atoms are given in the form of the equivalent isotropic displacement parameter defined as $4/3[a^2\beta_{11} + b^2\beta_{22} + c^2\beta_{33} + ab(\cos\gamma)\beta_{12} + ac(\cos\beta)\beta_{13} + bc(\cos\alpha)\beta_{23}]$. Starred atoms were refined isotropically.

that the tungsten tetracarboxylates are susceptible to air oxidation while the molybdenum tetracarboxylates are relatively air-stable materials. Nor is it surprising that the reaction of molybdenum tetraacetate with trimethylsilyl chloride and dppm produces $Mo_2Cl_4(dppm)_2$ in high yield, yet the corresponding reaction using tungsten tetrabenzoate produces an oxidized species as evidenced by the visible absorption spectrum (496 nm) which is characteristic of $W_2Cl_4X_2(dppm)_2$ compounds (X = Cl, SPh, SePh) [7, 8]. The oxidizing ability of trimethylsilyl chloride is also seen in a similar visible spectrum (498 nm) from its reaction with the desired product, $W_2Cl_4(dppm)_2$. Thus the susceptibility of the W_2^{4+} core towards oxidation makes this particular route unusable.

The actual synthesis of $W_2Cl_4(dppm)_2$ followed the procedure used by Schrock *et al.* [2] in preparing similar tungsten(II) dinuclear species, namely, the substitution of four monodentate phosphines for two bidentate phosphines as shown

$$W_2Cl_4[P(n\text{-}Bu)_3]_4 + 2dppm \longrightarrow W_2Cl_4(dppm)_2 + 4P(n\text{-}Bu)_3$$

Unlike Schrock's $W_2Cl_4L_4$ and $W_2Cl_4(L{-}L)_2$ compounds, $W_2Cl_4(dppm)_2$ is prone to air oxidation. Traces of deaerated water, however, do not affect product formation, and, in fact, may hasten the reaction by reacting with the $P(n\text{-}Bu)_3$ as it is liberated, thus shifting the reaction equilibrium toward product formation. It is interesting to note that our preparation of $W_2Cl_4(dppm)_2$ is nearly identical to the reaction used by Walton to form the oxidized species $W_2(\mu\text{-}H)(\mu\text{-}Cl)Cl_4(dppm)_2$ [7]. The obvious high susceptibility of the $W_2Cl_4(dppm)_2$-W_2^{4+} core towards oxidation makes this compound a prime canditate for oxidative–addition studies. This possibility was one of the main reasons for preparing the compound and is currently being investigated in this laboratory.

Structure

The product, $W_2Cl_4(dppm)_2$, is a quadruply bonded dimer with a metal–metal bond length of 2.269(1) Å, which as expected, is slightly longer than that in the corresponding molybdenum analog at 2.138(1) Å [9]. The longer tungsten–tungsten vector can be attributed to the larger and more dense tungsten core which increases core–core repulsions and reduces the tungsten–tungsten orbital overlap, especially the overlap of the δ component. Unlike $Mo_2Cl_4(dppm)_2$, which has a crystallographically imposed inversion center, the crystallographic symmetry imposed upon $W_2Cl_4(dppm)_2$ is limited to a C_2 axis perpendicular to the metal–metal vector. This allows for internal rotation away from a strictly eclipsed rotational conformation about the metal–metal bond vector. Figure 2 illustrates this concerted effect by showing the projection down the metal–metal bond vector. Table IV contains the measured values for the four torsion angles, two of which are equivalent due to the symmetry imposing C_2 axis. The difference in magnitude between the three independent torsion angles can be viewed in terms of true internal rotation in combination with steric distortions to give an average twist of 17.25° from the eclipsed conformation. This too, would be expected to slightly increase the metal–metal bond distance, due in part, to a decrease in the δ overlap to 82% ($\cos 2\chi$) of its original value. In addition, the

TABLE III. Selected Bond Distances (Å) and Angles (°) for $W_2Cl_4(dppm)_2$

Atom 1	Atom 2	Distance	Atom 1	Atom 2	Atom 3	Angle
W	W'	2.269(1)	W'	W	Cl(1)	106.48(6)
W	Cl(1)	2.381(2)	W'	W	Cl(2)	109.28(7)
W	Cl(2)	2.371(2)	W'	W	P(1)	95.86(6)
W	P(1)	2.601(2)	W'	W	P(2)	95.71(6)
W	P(2)	2.519(2)	Cl(1)	W	Cl(2)	143.17(9)
P(1)	C(1)	1.853(9)	Cl(1)	W	P(1)	85.72(8)
P(1)	C(2)	1.820(10)	Cl(1)	W	P(2)	85.33(8)
P(1)	C(8)	1.835(9)	Cl(2)	W	P(1)	99.01(8)
P(2)	C(1)'	1.828(9)	Cl(2)	W	P(2)	82.71(8)
P(2)	C(14)	1.830(9)	P(1)	W	P(2)	167.00(8)
P(2)	C(20)	1.821(9)	W	P(1)	C(1)	110.0(3)
			W	P(2)	C(1)'	106.3(3)
			P(1)	C(1)	P(2)'	106.2(4)

[a]e.s.d.s given in parentheses.

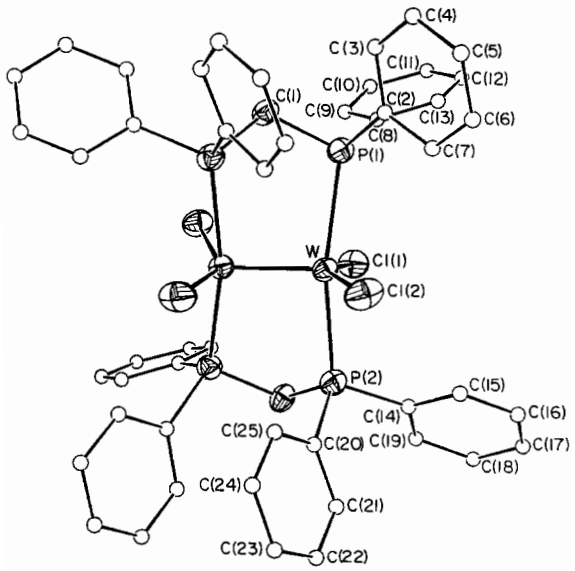

Fig. 1. Structure and labeling scheme for $W_2Cl_4(dppm)_2$. Atoms are represented by their 50% probability ellipsoids.

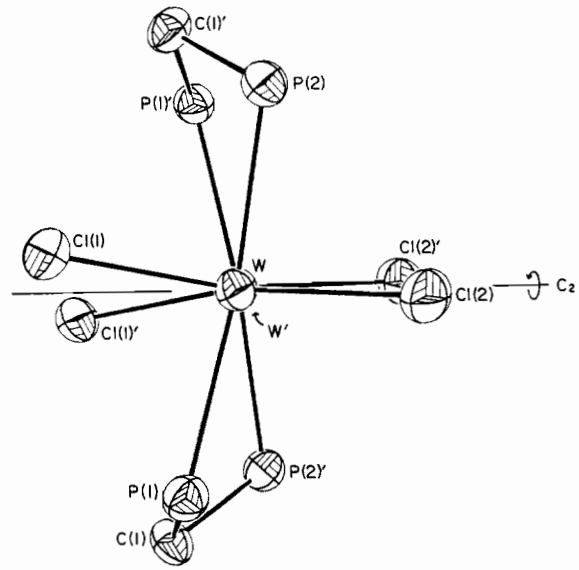

Fig. 2. Partial ORTEP plot of $W_2Cl_4(dppm)_2$ viewed down the W–W' axis illustrating the net torsion angle of 17.25°.

TABLE IV. Torsion Angles in $W_2Cl_4(dppm)_2$

Planes defining the angle		Torsion angles, χ (°)
Atoms in plane 1	Atoms in plane 2	
Cl(1), W, W'	W, W', Cl(1)'	21.9
Cl(2), W, W'	W, W', Cl(2)'	4.1
P(1), W, W'	W, W', P(2)'	21.5
P(2), W, W'	W, W', P(1)'	21.5
	χ_{ave} =	17.25

π component may also be affected by the rotation since four-fold axial symmetry down the tungsten–tungsten axis does not exist. The magnitude of this effect is dependent upon the differing ability of the phosphorus and chlorine ligands in interacting with the d_π tungsten orbitals.

Table V lists four sets of quadruply bonded tungsten and molybdenum dimers, their metal–metal bond distances and their average torsion angles [9–13]. It is interesting to note that the difference in metal–metal bond lengths between the molybdenum and tungsten analogs, ΔM–M, is approximately the same (0.133 Å) even when a difference in net torsion angle exists between the two dimers! It seems reasonable that the decrease in orbital overlap due to the torsion angle is less important in the W_2^{4+} core than in the Mo_2^{4+} core since the orbital overlap is already weakened from the greater tungsten–tungsten core repulsion. The existence of a torsion angle in W_2Cl_4-

TABLE V. M–M Bond Distances and Torsion Angles in $M_2Cl_4L_4$ and $M_2Cl_4(L-L)_2$ Compounds

	W–W (Å)	χ (°)	Mo–Mo (Å)	χ (°)	ΔM–M (Å)	Δχ (°)
$M_2Cl_4(dppm)_2$	2.269(1)	17.25	2.138(1)	0	0.131	17.25
β-$M_2Cl_4(dppe)_2$	2.314(1)	31.33	2.183(3)	30.5	0.131	0.83
α-$M_2Cl_4(dppe)_2$	2.280(1)	0	2.140(3)	0	0.140	0
$M_2Cl_4(PMe_3)_4$	2.262(1)	0	2.130(0)	0	0.132	0
					$\Delta M-M_{ave}$ =	0.133

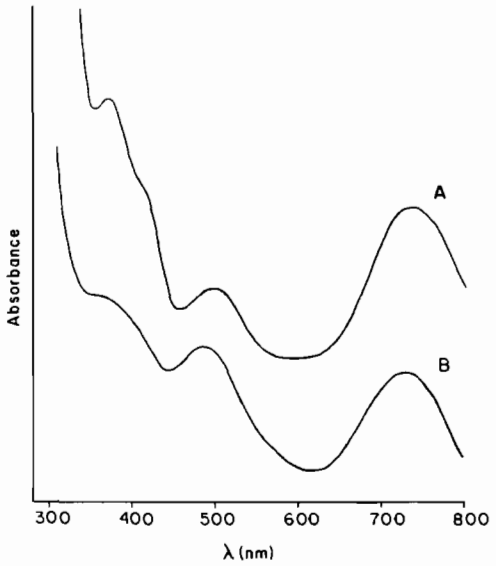

Fig. 3. Electronic absorption spectra of $W_2Cl_4(dppm)_2$; (A) benzene solution, (B) solid-state Nujol mull.

$(dppm)_2$ is the result of a balancing between maximum metal–metal orbital overlap, and minimum steric interaction from the dppm ligands which would prefer to be fully staggered as in the electron-rich triply bonded dimer, $Re_2Cl_4(dppm)_2$ [14]. As a result of internal crowding by the dppm ligands, appreciable distortions beyond the torsion angle occur. While the W–W–P angles are approximately equal, the W–P bond lengths differ by 0.082(2) Å. In $Re_2Cl_4(dppm)_2$, this difference is only 0.006(2) Å since steric interactions are relieved by the 45° torsion angle. Both $W-P_{ave}$ (2.56 Å) and $W-Cl_{ave}$ (2.38 Å) bond distances in $W_2Cl_4(dppm)_2$ are typical of $W_2Cl_4P_4$ group complexes and are slightly shorter (*ca.* 0.02 Å) than those found for their molybdenum counterpart, $Mo_2Cl_4(dppm)_2$.

Electronic Spectra

The solution (A) and solid-state (B) visible spectra of $W_2Cl_4(dppm)_2$ are illustrated in Fig. 3. The two highest electronic energy absorption bands (367 nm, 407 nm) in the solution spectrum are observed as one broad band in the solid-state spectrum at approximately 380 nm. The remaining two peaks in the solution spectrum are roughly 10 nm lower in energy than the corresponding peaks found in the solid-state spectrum. The lowest energy electronic absorption band (A: 737 nm, B: 726 nm) assigned to the $\delta \rightarrow \delta^*$ transition, exhibits a red shift of about 90 nm as compared to the value of the $\delta \rightarrow \delta^*$ transition in $Mo_2Cl_4(dppm)_2$ [15]. This corresponds to a weaker tungsten–tungsten bond as is observed crystallographically.

Supplementary Material

Full listings of bond angles, bond distances, and anisotropic displacement parameters (4 pages); and tables of observed and calculated structure factors (14 pages) are available. Copies may be obtained from F.A.C.

Acknowledgment

We thank the National Science Foundation for support.

References

1 F. A. Cotton and R. A. Walton, 'Multiple Bonds Between Metal Atoms', Wiley Interscience, New York, 1982, Chap. 3.1, and refs. therein.
2 R. R. Schrock, L. G. Sturgeoff and P. R. Sharp, *Inorg. Chem.*, *22*, 2801 (1983).
3 F. A. Cotton and W. Wang, *Inorg. Chem.*, *23*, 1604 (1984).
4 See, for example, A. Bino, F. A. Cotton and P. E. Fanwick, *Inorg. Chem.*, *18*, 3358 (1979).
5 F. A. Cotton, J. L. Hubbard, D. L. Lichtenberger and I. Shim, *J. Am. Chem. Soc.*, *104*, 679 (1982).
6 T. C. Zietlow, D. D. Klendworth, T. Nimroy, D. J. Salmon and R. A. Walton, *Inorg. Chem.*, *20*, 947 (1981).
7 P. E. Fanwick, W. S. Harwood and R. A. Walton, *Inorg. Chem.*, *26*, 242 (1987).

8 J. A. M. Canich and F. A. Cotton, unpublished results.
9 E. H. Abbott, K. S. Bose, F. A. Cotton, W. T. Hall and J. C. Sekutowski, *Inorg. Chem., 17*, 3240 (1978).
10 F. A. Cotton, T. R. Felthouse and D. G. Lay, *J. Am. Chem. Soc., 102*, 1431 (1980).
11 P. A. Agaskar and F. A. Cotton, *Inorg. Chem., 23*, 3383 (1984).
12 P. A. Agaskar and F. A. Cotton, *Inorg. Chem., 25*, 15 (1986).
13 F. A. Cotton, M. W. Extine, T. R. Felthouse, W. S. Kolthammer and D. G. Lay, *J. Am. Chem. Soc., 103*, 4040 (1981).
14 T. J. Barder, F. A. Cotton, K. R. Dunbar, G. L. Powell, W. Schwotzer and R. A. Walton, *Inorg. Chem., 24*, 2550 (1985).
15 N. F. Cole, D. R. Derringer, E. A. Fiore, D. J. Knoechel, R. K. Schmitt and T. J. Smith, *Inorg. Chem., 24*, 1978 (1985).